

1
2
3
4
5
6
7
8
9
10
11
12
13
14
15
16
17
18
19

Supplementary Material

***In vitro* studies of DNA condensation by bridging protein in a crowding environment**

SK Ramisetty, P. Langlete, R. Lale, R.S. Dias

FCS curve fitting procedure and parameters

The external detectors are from PicoQuant, and both were controlled by computer via the producer-developed softwares, Leica Application Suite X for microscope control and imaging, and SymphoTime for FCS data acquisition and processing. The minimal lag time was set to 0.003 ms. For FCS, a minimum of 6 recordings with a duration of 90 seconds were executed, with $\kappa = z_0/w_0 = 4.0$ for DNA. This protocol, combined with the use of weighted arithmetic means for data analysis gave a lower error, without much subjective influence on the results. The effective focal volume was set to the default 1 fl during curve fitting, as normalized data were sufficient. The curve-fitting algorithm tends to give a high triplet-state relaxation time, often above 40 ns, and had to be adjusted manually to a more realistic number, closer to 10 ns.

20 The number of species for all DNA samples was assumed to be two, where the slower one of higher
21 concentration was the DNA-dye-protein complex, and the resolution of the autocorrelation
22 function was maximized.

23 The process of calculating weighted means using bootstrapping is shortly described, as follows: a
24 recording is taken of the sample for 10 minutes; this is chopped into 6 intervals of approximately
25 90 seconds (in symphotime). For each of these, an autocorrelation function is constructed at
26 maximum resolution and a lag time of 0.003 ms (symphotime). A curve fit is done with the
27 assumption of two species and the triplet-state relaxation time manually set to 10 ns (symphotime).
28 The resulting curve fit gives us the diffusion time of the two species where the slower one is our
29 DNA. A "bootstrap" analysis is done on the curve fit (symphotime), and this gives us a standard
30 deviation for the diffusion time of our species for that single 90 second interval. Then weighted
31 arithmetic mean is calculated for all the six diffusion times by using the standard deviations from
32 the bootstrap analysis.

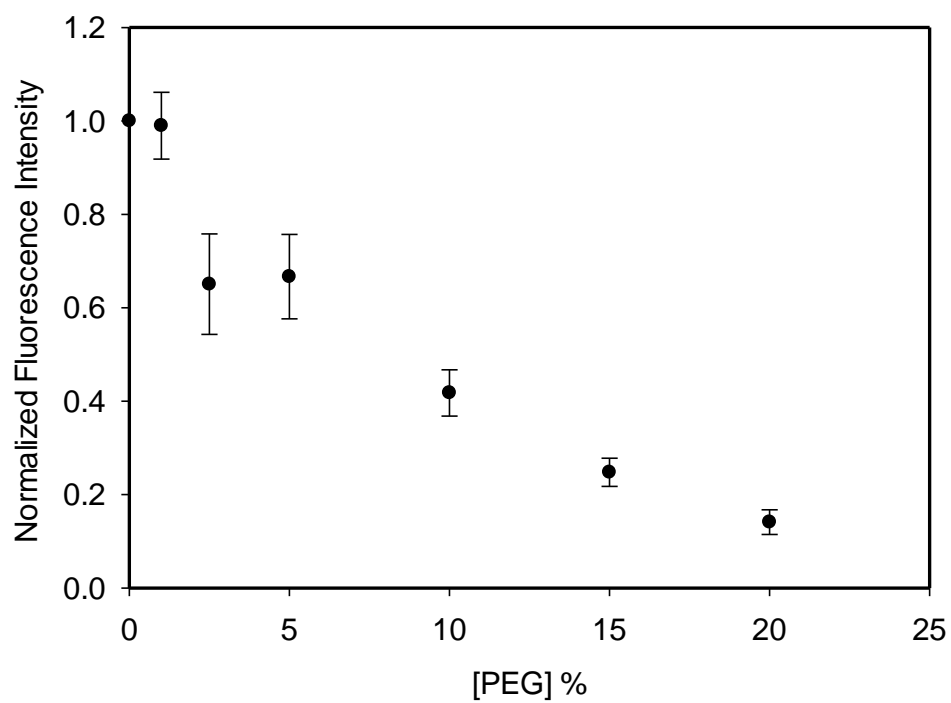
33

34 **Dye exclusion studies of DNA-PEG**

35 Dye exclusion studies for plasmid DNA and PEG were performed using protocol as described
36 previously [1].

37 In short, steady state fluorescence spectra were recorded using the Tecan Infinite 200-PRO
38 multifunctional plate reader. The fluorophore used for DNA was Gelstar nucleic acid stain (Lonza),
39 which has an emission maximum (λ_{em}) at 527 nm and an excitation maximum (λ_{ex}) at 493 nm in
40 the presence of DNA. In order to optimize the quality of the measurement, the 10,000×
41 concentrated stock solution of Gelstar was diluted to 10× as final working concentration.

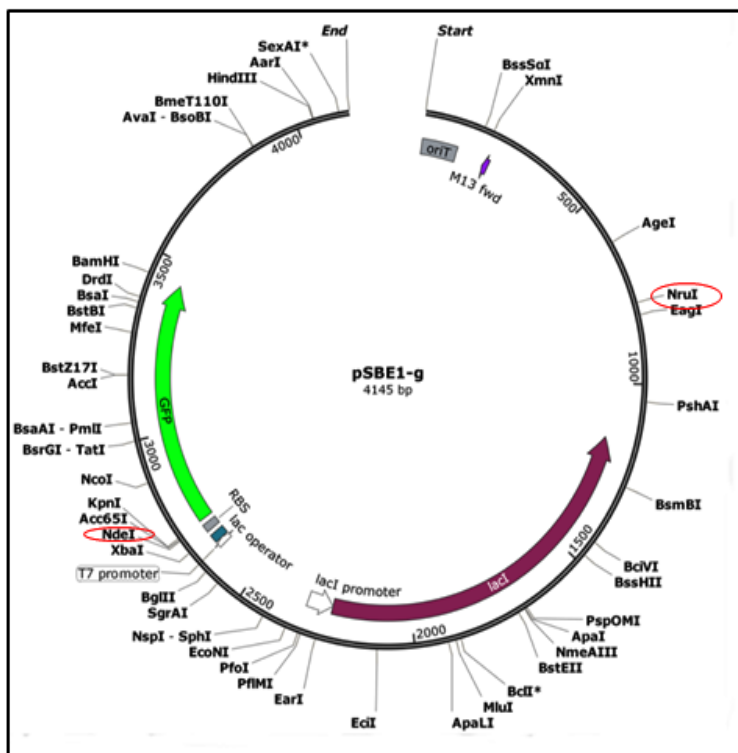
42



43

44 **Figure S1.** Fluorescence intensity of DNA–Gelstar complexes normalized to the fluorescence
45 intensity of DNA–Gelstar complexes in the absence of PEG, I/I_0 , shown as a function of PEG
46 concentration. The final concentration of DNA was 2 $\mu\text{g/mL}$.

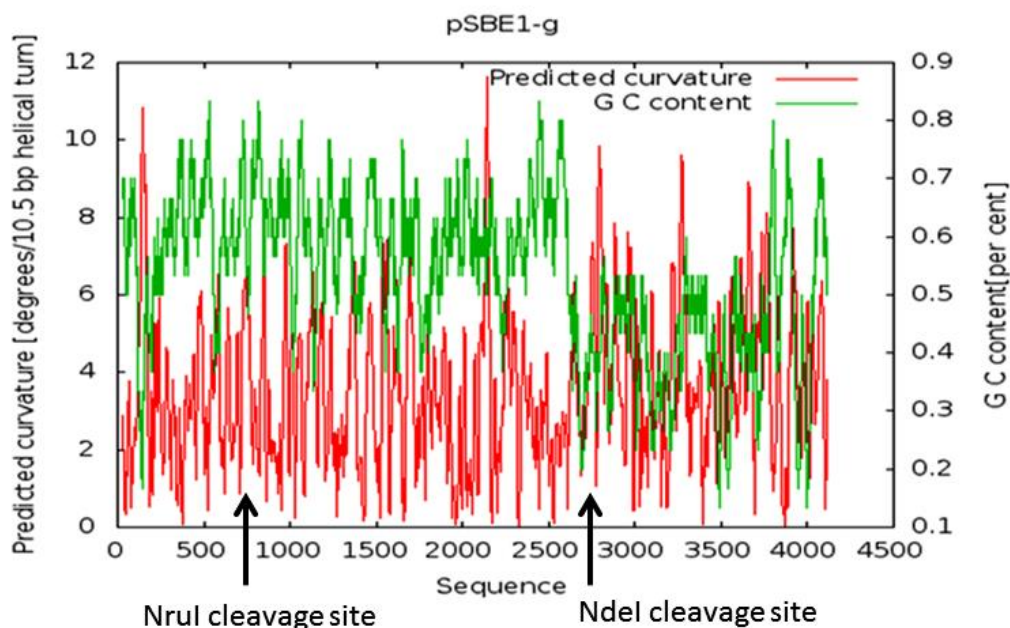
47



48
 49 **Figure S2.** The map of the amplicon (4145bp) carrying a T7 promoter. The recognition sites of
 50 the restriction enzymes used in this work are highlighted. Map is regenerated by Snap Gene Viewer
 51 software

52

53



54
55
56 **Figure S3.** DNA curvature prediction: Predicted DNA curvature (red) and GC content (green) of
57 pSBE1-g. Generated using Bend.it software.

58
59
60 **In vitro transcription and translation assay**
61 Production of green fluorescent protein (GFP) in the presence and absence of H-NS and PEG was
62 followed using an *in vitro* translation assay, TnT® Quick Coupled Transcription/Translation
63 Systems (Promega). For this assay, samples containing fixed concentrations of plasmid DNA (2
64 µg/mL) were premixed with varied concentrations of H-NS and PEG, as described above. The
65 equilibrated DNA–H-NS–PEG mixtures were transferred to vials containing the
66 translational/transcription master mix followed by the addition of methionine, required for *in vitro*
67 translation, according to the manufacturer’s protocol. Reactions were incubated for 1 h at 37 °C

68 and GFP production was estimated using a fluorescence plate reader M200 Pro Tecan
69 Spectrophotometer.

70
71 As mentioned in the introduction, H-NS is known to play a vital role in regulating a wide variety
72 of genes across the genome of bacteria. In order to learn more about the gene regulatory role of H-
73 NS in cellular conditions, we performed *in vitro* transcription/translation assays of DNA–H-NS
74 complexes in both presence and absence of crowding agents. The results are compiled in the form
75 of a heat map in Table S1.

76

77 **Table S1.** Heat map showing the fluorescence intensities of GFP, I_{525} , normalized to fluorescence
78 intensity of GFP produced in the absence of H-NS and PEG, $I_{525,0}$.

80

[H-NS] / μ M	$I_{525}/I_{525,0}$				
	0% PEG	0.5% PEG	1% PEG	2% PEG	4% PEG
0.00	1.00 \pm 0.04	0.83 \pm 0.15	0.66 \pm 0.15	0.21 \pm 0.06	0.11 \pm 0.11
0.05	1.02 \pm 0.13	0.85 \pm 0.17	0.68 \pm 0.15	0.21 \pm 0.06	0.00 \pm 0.09
0.10	1.02 \pm 0.13	0.64 \pm 0.09	0.68 \pm 0.13	0.30 \pm 0.09	0.02 \pm 0.06
0.25	0.77 \pm 0.13	0.77 \pm 0.09	0.72 \pm 0.19	0.38 \pm 0.09	0.09 \pm 0.09
0.50	0.36 \pm 0.11	0.49 \pm 0.04	0.66 \pm 0.53	0.17 \pm 0.17	0.06 \pm 0.09
0.75	0.32 \pm 0.09	0.15 \pm 0.21	0.26 \pm 0.04	0.17 \pm 0.06	0.04 \pm 0.02
1.00	0.13 \pm 0.09	0.26 \pm 0.06	0.17 \pm 0.11	0.09 \pm 0.11	0.15 \pm 0.11

79
81 Excitation and emission wavelengths were 485 nm and 525 nm respectively. The indicated values are the
82 mean of three independent sample sets and errors indicate the standard deviation from the mean.

83

84 The second column in Table 2 refers to $\frac{I_{525}}{I_{525,0}}$ of GFP expression in the presence of H-NS only. It

85 is clear that increasing the protein concentration results in a decrease in GFP expression, in good
86 agreement with previous reports [2]. On the other hand, increasing PEG concentration in the
87 absence of H-NS (first row) also leads to a clear decrease in GFP production, as described
88 previously [3, 4].

89 Our focus is the combined role of H-NS and PEG on gene regulation. For this we tested series of
90 samples with DNA–H-NS complexes with varying concentrations of PEG, also compiled in Table
91 S1. The three independent sample sets performed for these experiments showed a relatively large
92 variability, as reflected on the large errors of some of the points in Table S1. The synergism of H-
93 NS and PEG on gene regulation is therefore not obvious from the data, except for the samples
94 prepared with 0.1 μ M of H-NS and 0.5 % of PEG, where there is a clear decrease in the GFP
95 expression when compared to the sets prepared in the presence of only H-NS or PEG.

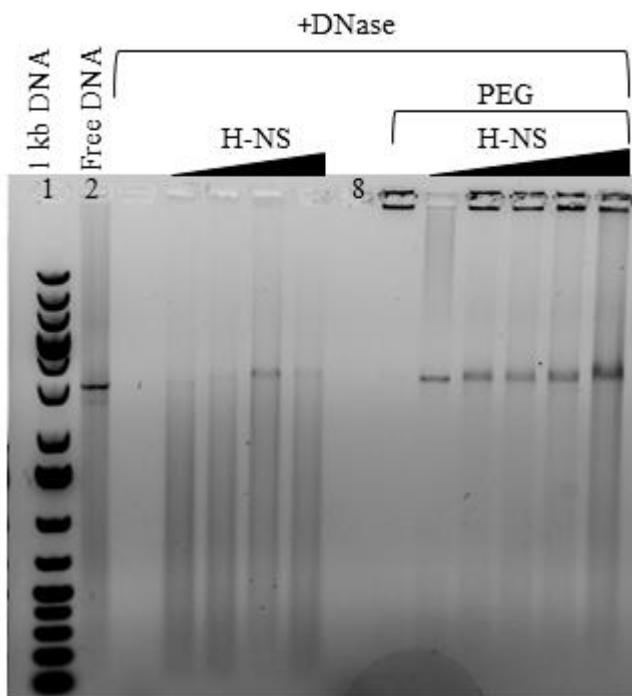
96

97 **DNase digestion of DNA-H-NS-PEG in the absence of Mg^{2+}**

98 In order to check the binding affinity of H-NS to DNA in the absence of Mg^{2+} , DNase digestion
99 assay was performed without $MgCl_2$. DNA–H-NS–PEG complexes were prepared as mentioned
100 in materials and methods sections, except that binding buffer has no $MgCl_2$. Once formed
101 complexes were treated with DNase enzyme and incubated for at least 20 minutes at 37 °C.

102 Fig S4 shows DNase digestion assay for DNA–H-NS–PEG complexes prepared without $MgCl_2$ in
103 the binding buffer. We observe a partial protection of DNA from DNase in the presence of H-NS
104 (see lane 4-7). Lane 9 shows the DNase digestion of DNA in the presence of 5% PEG. Addition
105 of H-NS leads to near complete protection of the DNA, showing that the synergism of PEG in H-
106 NS binding to DNA, and consequent protection towards DNase activity, is not affected by the
107 presence of Mg^{2+} , although the binding mechanism of H-NS to DNA is different (see discussion
108 in the paper). Fig S4 shows DNase digestion assay for DNA–H-NS–PEG complexes prepared
109 without $MgCl_2$ in the binding buffer. We observe a partial protection of DNA from DNase in the
110 presence of H-NS (lanes 4 to 7). Lane 9 shows the DNase digestion of DNA in the presence of
111 5% PEG. Addition of H-NS (lanes 10 to 14) leads to near complete protection of the DNA, showing

112 that the synergism of PEG in H-NS binding to DNA, and consequent protection towards DNase
 113 activity, is not affected by the presence of Mg^{2+} , although the binding mechanism of H-NS to DNA
 114 is different (see discussion in the paper).



115

Figure S4. DNase I protection assay in the absence of $MgCl_2$: To examine binding activity of H-NS to linear plasmid DNA in the absence of Mg^{2+} , DNase I digestion reactions were carried out at increasing concentrations of H-NS (0.5, 1, 5, 10, 25 μ M) in the absence (lanes 3 to 7) and presence of 5 % PEG (lanes 9 to 14). Lane 2 and 3 correspond to controls of free DNA with and without enzyme addition, respectively, and the last lane, 9, shows the digestion of DNA in the presence of 5 % PEG only. A final concentration of 5 μ g/mL of linear plasmid DNA was used for all reactions. Lane 8 was left unloaded.

116

117 References

- 118 1. Ramisetty, S. K., and R. S. Dias. 2015. Synergistic role of DNA-binding protein and
 119 macromolecular crowding on DNA condensation. An experimental and theoretical
 120 approach. *Journal of Molecular Liquids* 210, Part A:64-73.
- 121 2. Hommais, E. Krin, C. Laurent-Winter, O. Soutourina, A. Malpertuy, J.-P. Le Caer, A.
 122 Danchin, P. Bertin, Large-scale monitoring of pleiotropic regulation of gene expression by
 123 the prokaryotic nucleoid-associated protein, H-NS, *Molecular Microbiology* 40(1) (2001)
 124 20-36.

- 125 3. C. Tan, S. Saurabh, M. Bruchez, R. Schwartz, P. LeDuc, Molecular crowding shapes gene
126 722 expression in synthetic cellular nanosystems, *Nature nanotechnology* 8(8) (2013) 602-
127 608. 723
- 128 4. X. Ge, D. Luo, J. Xu, Cell-Free Protein Expression under Macromolecular Crowding 724
129 Conditions, *PLoS ONE* 6(12) (2011) e28707.